INVESTIGATION OF INDICATORS IN AEROGELS AND XEROGELS

By

Rebecca L. Wolfe

****

Submitted in partial fulfillment

of the requirements for

honors in the Department of Chemistry

UNION COLLEGE

March, 2003

ABSTRACT

WOLFE, REBECCA L. Investigation of indicators in aerogels and xerogels. Department of Chemistry, March 2003.

A sol-gel is a silicon-oxygen matrix that is suitable for the entrapment of chemical species, including biological species, indicators, dyes, and sensors. Aerogels are sol-gels prepared by supercritical extraction, whereas xerogels are allowed to dry under ambient conditions. The resulting materials differ considerably in their physical properties. We are investigating a series of luminescent species for use as probes of the microenvironment in different sol-gel maerials. Sol gels containing each probe are prepared as both xerogels and aerogels; aerogels are formed using a novel contained mold process. Spectral properties, including absorption or excitation spectra, emission spectra, time-based fluorescence scans, and fluorescence lifetime, of the entrapped probes are measured.

The research focuses on two dyes, tris(2,2'-bipyridyl)ruthenium(II), an oxygen sensor referred to as $Ru(bpy)_3^{2+}$, and Eosin-Y, a pH-indicator. Eosin-Y is successfully entrapped in xerogels and can be used to differentiate between xerogel materials, but does not survive the aerogel formation process. The response times of Eosin-Y-doped xerogels and pin-printed sol-gel microsensors to changes in pH are also investigated. The doped xerogels have relatively long response times of 20 minutes. Microsensors are expected to have shorter response times. Aerogels and xerogels doped with $Ru(bpy)_3^{2+}$ have similar excitation spectra, with maxima at 470 nm, with xerogels having enhanced intensity. The $Ru(bpy)_3^{2+}$-doped materials differ in the shape of their emission bands, with emission maxima ranging from 590 to 604 nm. Lifetime data for aerogels and xerogels doped with $Ru(bpy)_3^{2+}$ differ indicating that the species is entrapped in different microenvironments. $Ru(bpy)_3^{2+}$-doped aerogels are successfully used as oxygen sensors and demonstrate response times of approximately 3 seconds.

ACKNOWLEDGMENTS

This research would never have been accomplished so successfully without the help of Professor Mary Carroll whose guidance and support went above and beyond the realm of chemistry. I would also like to extend my gratitude to Professors Michael Hagerman of the Union College Chemistry Department and Ann Anderson of the Union College Mechanical Engineering Department who brought wisdom and insight every week to our aerogel meetings. It is important to acknowledge the helpful contributions of fellow students Desiree Plata and Yadira Briones of the Chemistry Department, Ben Gauthier, Smitesh Bakrania, and Matt King of the Mechanical Engineering Department, and Sheila Anane of Cornell University. Also, without the help of the extensive knowledge and patient guidance of the Union College Chemistry faculty I would never have been able to complete this research.

In terms of funding, I would like to thank the Union College Chemistry Department, the Internal Education Foundation, the Surdna Summer Research Fellowship, the Eli Lilly Women Chemists Committee Travel Grant, and the National Science Foundation. All of these organizations contributed to various parts of my research including my working at Union College this past summer, the instrumentation I was able to use, and my presentation at the 225th National American Chemical Society Meeting in New Orleans.

I would like to express my gratitude to my friends and family whose unconditional support helped carry me through this research. With my family and friends encouraging me every step of the way, it was easy to stay focused on the ultimate goals of my research.

Finally, I would like to wish all my fellow chemistry and biochemistry classmates who have helped keep me sane while I was at Union College the best of luck in their future endeavors.

Rebecca L. Wolfe

TABLE OF CONTENTS

TABLE OF FIGURES

TABLE OF TABLES

INTRODUCTION

Introduction to Sol Gels

A sol gel is a silicon-oxygen matrix that is suitable for the entrapment of chemical species, including biological species, indicators, dyes, and sensors. It is formed by means of a combination hydrolysis and condensation reaction at room temperature[1]:

$$Si(OR)_4 + nH_2O \rightarrow Si(OR)_{4-n}(OH)_n + ROH \quad \text{hydrolysis}$$

$$Si\text{-}OH + RO\text{-}Si \rightarrow Si\text{-}O\text{-}Si + ROH \quad \text{condensation}$$

$$Si\text{-}OH + HO\text{-}Si \rightarrow Si\text{-}O\text{-}Si + H_2O \quad \text{polycondensation}$$

This research paper focuses on two forms of the sol gel: the xerogel and the aerogel. A xerogel is a porous solid created by drying a gel under subcritical conditions. An aerogel is also a porous solid produced from a gel, but with much less shrinkage than a xerogel. An aerogel is created by supercritical extraction of solvent[2]. Aerogels are made up of 90-99% air, having the lowest density of any known solid[3]. Aerogels have been fascinating researchers and space engineers with their remarkable physical properties. They are particularly well-known for their incredible insulating properties with regard to thermal, electrical and acoustic energy transfers[4]. They have even been used by NASA to capture cosmic dust[5]. Figure 1 shows a simplified diagram of the sol-gel process on which my study focuses.

There are many advantages to using sol-gel material. Sol-gel derived inorganic glasses have thermo-mechanical and optical advantages over gelatin films and boric acid glasses. They are also much more processible,

and organic and inorganic dopants are easily introduced in to the sol-gel matrices[6]. Sol gels can also be used to create alternative formats besides glasses. Other than aerogels and xerogels, extensive research has been done on sol-gel derived thin films, monoliths, ormosils, and optical fibers, among other materials.

To examine fluorescent probes within sol-gel materials, the materials are doped with fluorescent dyes prior to gelling. There are many interesting motivations for doping the sol gels. One main purpose is to explore the mobility of the fluorescent probe within the sol-gel material to examine solvent motion, association of the probe with the pore walls of the material, molecule-matrix interactions, environmental heterogeneity, phase segregation, surface chemistry, and internal solvent and dopant dynamics[7]. Another important reason for doping sol gels is the application of indicators entrapped within the sol-gel materials as chemical sensors.

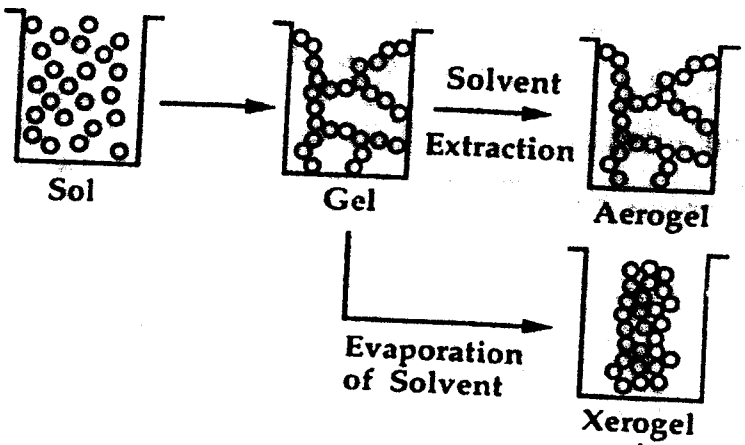

Figure 1. Sol-Gel Process adapted from Figure 1 in Brinker and Scherer Sol-Gel Science[4]

Introduction to Fluorescence and Absorbance

To measure how the probes interact within the sol-gel matrices, their fluorescence and absorption properties were monitored. The probes in solutions, xerogels, and aerogels were then compared with each other as well as literature values from analogous experiments. UV/Visible Absorption spectra were utilized to measure at what wavelength and to what extent the dye within the sol gel absorbed the light passing through it. Fluorescence emission and excitation spectra were examined to provide information on the effect of the various sol-gel matrices on the fluorescent properties of the dyes. In this research, lifetime measurements were used for studying the possible energy transfers and quenching of the $Ru(bpy)_3^{2+}$ moiety doped within xerogels and aerogels. Lifetime measurements were also used to investigate the solvent rigidity and environmental homogeneity of the xerogels and aerogels[7].

The modified Jablonski diagram[8] seen in Figure 2 can be used to explain absorption and fluorescence. A chemical species always prefers to be in its lowest energy level. In the Jablonski diagram (Figure 2), the lowest energy states are found in the ground state, represented by S_0. When the chemical species absorbs a photon, a valence electron moves from one orbital to another higher orbital. The species is then promoted to an excited state, represented by S_1 in the diagram. Once the species is in the excited state it returns back down to the ground state by giving off energy. There are

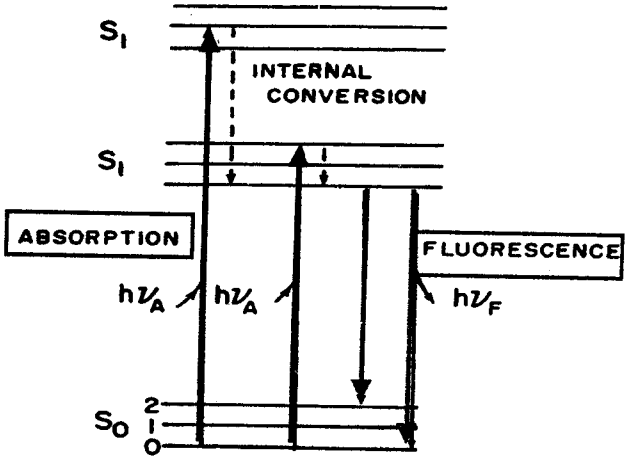

Figure 1.3. Jablonski diagram.

Figure 2. Jablonski diagram for absorbance and fluorescence only; where S_0 = singlet ground state, S_1 = singlet excited state, v_A = frequency of absorbed photon, and v_F = frequency of fluorescence adapted from Figure 1.3 in Lakowicz Principles of Fluorescence Spectroscopy[8]

several methods of returning to the ground state, but this research focuses on giving off energy through the fluorescence process. Fluorescence is an advantageous method for examining the sol gels because it reports on the nature of the local microenvironments surrounding the probe molecule within the sol-gel materials[7].

Absorbance for the probes being studied follows Beer's Law:

$$A = abc \qquad \text{(Equation 1)}$$

where A is absorbance, a is absorptivity, b is pathlength, and c is concentration. Thus the absorbance is linearly proportional to the probe concentration. Absorbance can be represented by the following equation:

$$S + h\nu \rightarrow S^* \qquad \text{(Equation 2)}$$

where S is a singlet state (all electron spins are paired), $h\nu$ is the photon of light being absorbed, and S* is a high energy, excited singlet state. Absorbance is a very fast process, occurring on the order of 10^{-14} to 10^{-15} seconds, so there are few competing factors with the process.

Fluorescence is a process in which the excited state molecule moves down to the ground state level by emitting a photon of light. This process can be represented by the following equation:

$$S^* \rightarrow S + h\nu \qquad \text{(Equation 3)}$$

Fluorescence emission and excitation spectra can be used to investigate the dye within the sol gel. Emission scans measure at what wavelengths the dye fluoresces and to what extent. Excitation scans measure the wavelength at

which the dye excites and, thus, absorbs light. Instead of measuring the extent of the absorption, it measures the extent the species fluoresces following excitation. Excitation maxima and absorption maxima should thus occur at the same wavelength. Because fluorescence and absorbance are directly related, fluorescence is also linearly proportional to concentration (as long as $A < 0.05$)[9].

Lifetime measurements can be used to measure decay of fluorescence intensity of a molecular species. The lifetime is the average time that a molecule spends in the excited state before emitting a photon and returning to the ground state. Fluorescent lifetime measurements can be represented in the following equation:

$$I(t) = A_1 e^{-t/\tau} \quad \text{(for a single exponential model)} \qquad \text{Equation 4}$$

$$I(t) = A_1 e^{-t/\tau_1} + A_2 e^{-t/\tau_2} \quad \text{(for a double exponential model)} \qquad \text{Equation 5}$$

where I(t) represents the fluorescent intensity at time t, A_1 and A_2 represent the pre-exponential factors, and τ^1 and τ^2 represent the lifetimes.

Once a molecule absorbs a photon of light, there are several competing processes through which the molecule can release the energy. Fluorescence, the process described in Equation 3, is one such process. However, there are many other processes. Lifetime measuements take into account these other processes, particularly possible energy transfers and quenching. These two possibilities are represented by electronic energy transfer and collisional deactivation, respectively. Electronic energy transfer can be represented in the following equation:

$$S^* + S \rightarrow S + S^* \qquad \text{(Equation 6)}$$

The process of collisional deactivation, or quenching, can be represented in the following equation:

$$S^* + M \rightarrow S + M \qquad \text{(Equation 7)}$$

where M is a body that carries thermal energy.

Introduction to Eosin-Y

For the first half of the research project, the pH indicator Eosin-Y, a pink-orange dye whose structure is shown in Figure 3, was used. Eosin-Y can be used as a pH indicator in solutions ranging from pH values of 1.0 to 3.0. From the structure shown in Figure 3, it can be seen that Eosin-Y contains a carboxylic group and a hydroxyl group; these have pKa values of 3.25 and 3.80, respectively.

The goals of this part of the thesis research were to prepare and evaluate the spectral properties of Eosin-Y entrapped in sol-gel matrices in order to demonstrate the utility of the immobilized Eosin Y as a pH sensor and also to further gain an understanding of the sol-gel matrix. I investigated how Eosin-Y reacted with acids and bases once it was entrapped in a silicon-oxygen matrix. Fluorescence and absorption measurements were used to see how the dye and the xerogels interacted with each other. Through the results of these experiments, I was able to demonstrate the utility of the Eosin-Y-doped sol gel as a sensor and gain an understanding of the sol-gel environment.

For one week during the summer of 2002, a part of this research was conducted in Professor Frank Bright's laboratory at the State University of New York at Buffalo with his research group and instrumentation. The Eosin-Y-doped sol-gel material was transferred onto microscope slides, and the slides were imaged onto a computer screen to show the extent of fluorescence. Although the time spent in Buffalo was brief, it was interesting and helpful.

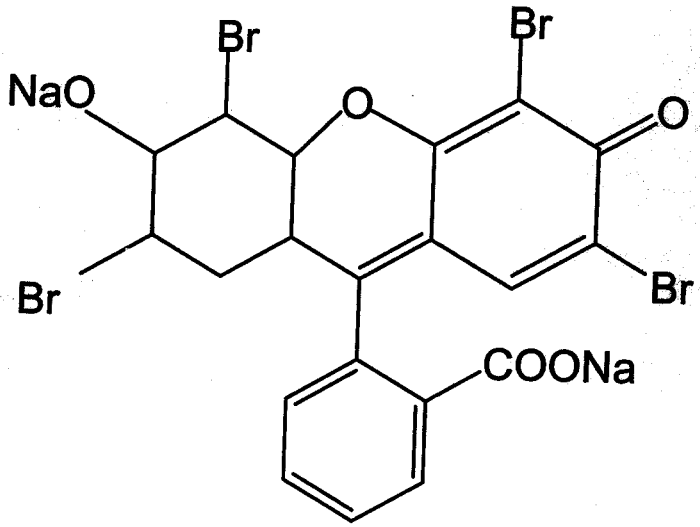

Figure 3. Structure of Eosin-Y

Introduction to $Ru(bpy)_3^{2+}$

For the second half of the research project, the focus was shifted to the probe tris(2,2'-bipyridyl)ruthenium(II), or $Ru(bpy)_3^{2+}$. This probe is a ruthenium complex where "bpy" represents the bipyridine ligand. The structure of $Ru(bpy)_3^{2+}$ can be seen in Figure 4. $Ru(bpy)_3^{2+}$ is often used in the study of sol gels as a probe to examine the mobility in polar regions of glass, the mobility of entrapped solvents, the accessibility to oxygen gas, and the development of the matrix[10]. There has been much research on ruthenium complexes in studies of organometallic molecules due to their luminescence properties with long excited state lifetimes, redox properties, excited state reactivities, and relatively high chemical and thermal stability[10].

From previous research[10] of $Ru(bpy)_3^{2+}$ in sol-gel materials, it has been demonstrated that $Ru(bpy)_3^{2+}$ shows an intense absorption band at 450 nm and a shoulder at 420 nm. Both of these peaks can be attributed to metal-to-ligand charge transfer (t_{2g} (Ru) $\rightarrow \Pi^*$ (bpy) transitions). Smaller bands or shoulders exhibited at 325 and 350 nm are assigned to metal centered d-d transitions. There is also an intense band at 285 nm that is due to ligand centered ($\Pi \rightarrow \Pi^*$) transitions. In fluorescence spectra, it has been shown that $Ru(bpy)_3^{2+}$ in sol-gel materials shows emission maxima at 600-620 nm. These maxima can be attributed to emission from the triplet metal-to-ligand charge transfer excited state to the ground state. Red and blue shifts in fluorescent spectral data have been observed for $Ru(bpy)_3^{2+}$ entrapped in sol-gel materials[10].

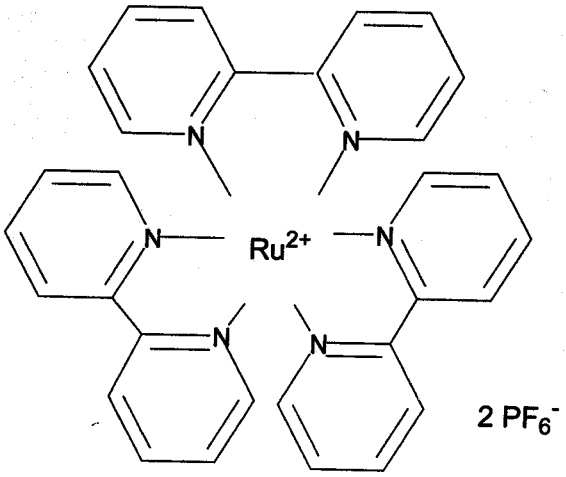

Figure 4. Structure of $Ru(bpy)_3^{2+}$

The goal of the research involving the $Ru(bpy)_3^{2+}$ probe was to evaluate $Ru(bpy)_3^{2+}$-doped aerogels and corresponding $Ru(bpy)_3^{2+}$-doped xerogels in terms of fluorescence emission and excitation, and fluorescence lifetime. Evaluation of how the ruthenium complex's properties may have changed in response to the changes in structure and chemistry of the gel matrix was conducted. The aerogels and xerogels were made by Professor Ann Anderson, Ben Gauthier, Smitesh Bakrania, and Matt King of the Union College Mechanical Engineering department. A collaboration was established with the mechanical engineers who are developing a patent to a new process for a faster, easier way to create aerogels. The research project also included a collaboration with Professor Michael Hagerman, an inorganic chemist at Union College, who is investigating ruthenium complexes trapped in thin films of clays. A possible model obtained from literature[10] on how $Ru(bpy)_3^{2+}$ is entrapped inside the silicon-oxygen matrix is shown in Figure 5.

A final goal involving $Ru(bpy)_3^{2+}$ was to evaluate $Ru(bpy)_3^{2+}$-doped aerogels as oxygen sensors. The fluorescence of $Ru(bpy)_3^{2+}$ in solution is quenched with oxygen, however, it was unknown whether the $Ru(bpy)_3^{2+}$ entrapped in aerogels would be as competent as an oxygen sensor as free, mobile $Ru(bpy)_3^{2+}$ in solution.

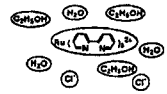

(a) Sol

5a. $Ru(bpy)_3^{2+}$ complexes are surrounded by the solvent molecules. The solvent molecules are free to rotate upon excitation of the complexes[10].

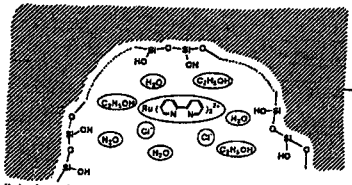

(b) As-deposited

5b. The solvent molecules continue to surround the $Ru(bpy)_3^{2+}$ complexes. They interact strongly with the silanol groups of the gel, thus rotation is restricted[10].

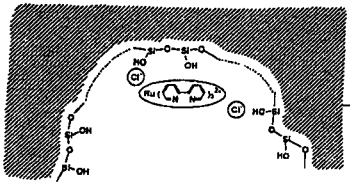

(c) Up to 200°C

5c. The solvent in the gel pores evaporates. Through direct interaction with the oxygen of the silanol groups and/or siloxane chains, the complexes are able to weakly bind to the gel network[10].

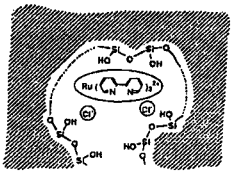

(d) Over 200°C

5d. Gel pores collapse due to condensation reactions between the silanol groups. The complexes become almost fully entrapped in the gel network[10].

Figure 5. Illustration on the process of the entrapment of $Ru(bpy)_3^{2+}$ in the sol-gel material adapted from Figure 10 in Innocenzi, Kozuka, and Yoko *J. Phys. Chem. B*, 1997, 101, 2285-2291.

INTRODUCTION WORKS CITED

[1] Narang, U.; Wang, R.; Prasad, P.N.; Bright, F.V. *Journal of Physical Chemistry*, 1994, 98, 17-22.

[2] Ferraris, Chiari F. and Hackley, Vincent A. The Use of Nomenclature in Dispersion Science and Technology. 8/01. NIST. 7/14/02 http://www.nist/c ...ublic_affairs/practiceguide/SP960-3.pdf.

[3] Gauthier, Ben M. Enhanced Aerogel Fabrication. Mechanical Engineering at Union College. 7/14/2002 http://tardis.union.ed/me_dept/me_dept.html.

[4] Brinker, C. Jeffrey, and George W. Scherer. Sol-Gel Science. New York: Academic Press, 1989. 786.

[5] The Sol-Gel Gateway. "Sculpting Air." 2002. January 15, 2003. http://www.solgel.com/articles/dec02/aeroart.asp.

[6] Lam, Sio Kuan and Lo, Dennis. "Delayed Luminescence Spectroscopy and Optical Phase Conjugation in Eosin Y-Doped Sol-Gel Silica Glasses." *Chemical Physics Letters*. **1998**, *297*, 329-334.

[7] Keeling-Tucker, Tracey and Brennan, John D. "Fluorescent Probes as Reporters on the Local Structure and Dynamics in Sol-Gel-Derived Nanocomposite Materials." *Chem. Mater.* **2001**, *13*, 3331-3350.

[8] Lakowicz, Joseph R. Principles of Fluorescence Spectroscopy. New York: Plenum Press, 1983. 5.

[9] Rubinson, Kenneth A. and Rubinson, Judith F. Contemporary Instrumental Analysis. New Jersey: Prentice Hall, 2000. 304.

[10] Innocenzi, Plinio, Kozuka, Hiromitsu, and Yoko, Toshinobu. "Fluorescence Properties of the $Ru(bpy)_3^{2+}$ Complex Incorporated in Sol-Gel-Derived Silica Coating Films. *J. Phys. Chem. B*, 1997, 101, 2285-2291.

EXPERIMENTAL

There are seven parts of the experimental section of this research. They are (1) the preparation of xerogels, (2) the preparation of aerogels, (3) excitation and emission spectra, (4) UV/visible absorption spectra, (5) steady-state time-based fluorescence scans, (6) lifetime fluorescence decay curves, and (7) the experiments that were performed at the University of Buffalo.

Materials

The tetramethyl orthosilicate (TMOS), tetraethyl orthosilicate (TEOS), and trimethoxypropylsilane (n-Propyl TMOS) were all purchased from Aldrich and were all 98% pure. The Eosin-Y dye (a neutral molecule) was also purchased from Aldrich, but with an 89% purity. The Eosin-Y stock solution was prepared in deionized water. The $Ru(bpy)_3^{2+}\cdot 6H_2O$ dye was purchased from Strem Chemicals and was 98% pure with a counter ion of Cl^-. The $Ru(bpy)_3^{2+}$ stock solution was prepared in deionized water.

Preparation of Xerogels

The preparation of the Eosin-Y-doped xerogels was done in the chemistry department laboratory, whereas the $Ru(bpy)_3^{2+}$-doped xerogels were created by the mechanical engineers who also fabricated the aerogels.

Eosin-Y-doped Xerogels

To prepare the Eosin-Y-doped xerogels, a solution containing a silicon-oxygen precursor was created. The solution was then doped with Eosin-Y and poured in aliquots into cuvettes. The cuvettes were allowed to dry to form the xerogels. The first step in the whole process was to create the

solution using the given precursor. Three different precursors were used: tetramethyl orthosilicate (TMOS), tetraethyl orthosilicate (TEOS), and trimethoxypropylsilane (n-Propyl TMOS). The three precursors were used in three different recipes as shown in Table I. For each recipe, the precursor(s) and solvent were added to a beaker, then the solution was allowed to stir with a stir-bar until it became monophasic. The volume of Eosin-Y used in each solution depended on the desired concentration in the wet gel. Amounts varying from 5 μL to 50 μL of a 5.0×10^{-4} M aqueous solution Eosin-Y were added to the samples to produce the desired concentrations.

Once the solution became monophasic, each aliquot was doped with the desired amount of Eosin-Y to make xerogels of different indicator concentrations. Then the gels were allowed to dry in polystyrene cuvettes. The samples were dried for three days with a cuvette cap on. Then the cap was replaced with perforated parafilm to speed up the process. After approximately one week, the xerogels had pulled away from the walls of the cuvettes. After several weeks, the xerogels dried with approximately 60% shrinkage in total volume occurring. Continuous shrinkage occurred over time.

$Ru(bpy)_3^{2+}$-doped Xerogels

The $Ru(bpy)_3^{2+}$-doped xerogels were prepared by the mechanical engineers using the recipe shown in Table II. The amount of $Ru(bpy)_3^{2+}$ used in each solution depended on the desired concentration. When a certain volume of $Ru(bpy)_3^{2+}$ dye was added to the solution, it replaced that volume

of water in the recipe. The solutions gelled into "wet" xerogels overnight, meaning that although they were solid, the monoliths had not fully pulled away from the walls of the cuvettes. The solvent had thus not evaporated fully out of the gels. After approximately one week, the xerogels had pulled away from the walls of the cuvette. After several weeks, the xerogels dried fully with approximately 60% shrinkage in total occurring.

Preparation of Aerogels

The fabrication of the aerogels was performed by Ben Gauthier, Smitesh Bakrania, Matt King, and Professor Ann Anderson of the Union College Mechanical Engineering department. The biggest obstacle to creating the aerogels was that any surface tension in the gel would lead to fracture. Ben Gauthier, before he left Union for Stanford University's graduate school, had been developing a new technique to manufacture aerogels based on a contained mold process employing the supercritical state of a fluid. Smitesh Bakrania has continued Gauthier's work. Ideally, the technique will create aerogels within minutes as opposed to hours or days; however, my colleagues are still working on the amount of time required in the aerogel fabrication process. The fastest that they have been able to create a batch of aerogels has been five hours.

The recipe used for the fabrication of $Ru(bpy)_3^{2+}$-doped aerogels can be seen in Table III. The volume of $Ru(bpy)_3^{2+}$ used in each solution depended on the desired concentration. This is the same recipe that the mechanical engineers used to fabricate the xerogels, except instead of

pouring the solution into cuvettes, it was poured into a mold with different bores for each aerogel.

Excitation and Emission Spectra

For obtaining excitation and emission spectra, a PTI Quantamaster fluorometer was used. The polystyrene cuvette, which could contain a sol-gel solution, a xerogel, or an aerogel, was placed in the instrument. Tables IV and V contain the parameters used for excitation and emission spectra, respectively, of both Eosin-Y-doped and $Ru(bpy)_3^{2+}$-doped sol-gel materials. For emission and excitation spectra for both of the dyes, the excitation and emission slits were varied in length to improve the signal-to-noise (S/N) ratio for each concentration of the sample within the cuvette.

UV/Visible Absorption Spectra

For obtaining UV/visible absorption spectra, an HP 8453 UV-Visible Diode Array Spectrophotometer was used. The instrument was blanked with a polystyrene cuvette containing everything the sample contained excluding the dye. A cuvette containing the sample was then placed in the instrument and spectra were taken over a range of 250 nm to 800 nm.

Steady-State Time-Based Scans

Two different parts of this research project required the use of steady-state time-based scans. The two different experiments used two different fluorometers.

The steady-state time-based scans using Eosin-Y-doped xerogels used a PTI Quantamaster fluorometer. These scans were utilized to

demonstrate the pH indicator abilities of Eosin-Y entrapped in xerogels: whether it could detect changes in pH and whether it remained a reversible indicator. For the time-based scans of Eosin-Y-doped xerogels, the excitation wavelength was set for 525 nm, and the emission wavelength was set for 545 nm. One data point per second was recorded and the experiment duration was two hours. The excitation and emission slits were both set at 2 nm. At the beginning of each time-based scan, the xerogel was soaked in 1.000 mL of deionized water. Then alternating 100-μL aliquots of either 0.1 M HCl or 0.1 M NaOH were added every 15 minutes to the cuvette to observe the response of the pH sensor (Eosin-Y entrapped in the xerogel) to changes in pH.

The steady-state time-based scans involving $Ru(bpy)_3^{2+}$-doped aerogels used a PTI LaserStrobe Fluorescence Lifetime System. The purpose of this experiment was to evaluate $Ru(bpy)_3^{2+}$-doped aerogels as oxygen sensors. The steady-state time-based scans were performed at an excitation wavelength of 446 nm and an emission wavelength of 590 nm. The instrument took a measurment every 8 s for 360 s (or 6 min). The aerogel was first exposed to air for 30 seconds. Then, the aerogel in a cuvette was placed in the four-part turet of the instrument for fluorescence examination. The fluorescent intensity was measured for 2 min, then the instrument was paused, and nitrogen was pumped into the cuvette containing the aerogel through plastic tubing for 2 min. The instrument was again paused, and the top of the instrument was opened to allow the aerogel to become saturated

again with air. The fluorescence intensity was measured for another 2 min following the allowance of air.

Lifetime Fluorescence Decay Curves

For obtaining fluorescence decay curves, two different lifetime decay instruments were used.

For the first half of the research, a PTI LS-100 Fluorescence Luminescence System was used. This instrument was used with the $Ru(bpy)_3^{2+}$ samples to analyze the fluorescence lifetime decay of $Ru(bpy)_3^{2+}$ entrapped in different microenvironments. The samples were placed in fluorescence cuvettes polystyrene. One sample at a time was placed in position one in the four-holed turret in the instrument. Opposite from the sample was a fluorescence cuvette in position three filled with a light-scattering solution of Ludox® colloidal silica. The lifetime instrument uses a nitrogen-gas-filled lamp, so the excitation wavelength chosen must be one at which nitrogen emits. Consequently, the excitation wavelength and the scatterer wavelength were both set at 337 nm, and the emission wavelength, which was independent of the nitrogen gas, was set at 590 nm. The emission wavelength is not set to the maximum emission wavelength known for the samples because the instrument's detector was not red-sensitive, and thus a less optimal wavelength was chosen[1]. The parameters for the lifetime decay curves can be seen in Table VI. The start delay and end delay were 100 nanoseconds and 400 nanoseconds, respectively. For each scan, 100

channels were utilized, and the integration time was set 0.1 seconds. To increase the signal-to-noise ratio, 50 averages were done on each sample.

For the second half of the research, a newer instrument, the PTI LaserStrobe Fluorescence Lifetime System, was employed. This new lifetime decay instrument used a pulsed nitrogen-pumped dye double laser. The nitrogen laser was a PTI model GL-3300 and the dye laser was a PTI model GL-302. Because one part of the laser was a dye laser, an optimal emission wavelength of 446 nm could be used. The laser dye used was also from PTI, and it was labelled PLD446 Coumarin 450 1.0×10^{-2} M in ethanol. The parameters for decay curves of aerogels and xerogels with the new instrument can be seen in Table VI.

State University of New York at Buffalo Research

At the University at Buffalo, a sol-gel solution was prepared with the recipe found in Table VII. The solution was then doped with Eosin-Y so that the concentration was 3.0×10^{-6}M. The next step was to load 50.0 μL of the solution into a Printer-Cartesian Technologies MicroSys PA Series pin-printer. Five microscope slides were created with an array of sol-gel dots. The slides were aged for two days. Normally the research students at the University of Buffalo age their slides for two weeks; however, my research time there was limited and, consequently, I was forced to shorten the aging process.

The slides were then excited by a LiConix Helium Cadmium Laser, model 4220N. The slides were excited at 442 nm. A CCD camera with an exposure time of 1.000 seconds took pictures of the excitation and the

fluorescing images appeared on the computer. The first image was taken with the slide surrounded only by air. Then the slide was flooded with 0.1 M HCl, then 0.01 M NaOH, and finally deionized water with a pH of 5.5. The flooding was done to demonstrate how Eosin-Y acted as a pH indicator while entrapped in a sol-gel matrix pin-printed on a microscope slide. The changing of pH was done to test the reversibility of Eosin-Y as a pH sensor in the sol-gel.

Table I. Recipes for the preparation of Eosin-Y-doped xerogels

Precursors	Amounts Used (mL)	Solvents	Amounts Used (mL)	Recipe Obtained from	Time Allowed for Stirring
n-Propyl TMOS TMOS	8.70 8.70	DI[1] Water 1.0 M HCl Ethanol 5.0×10^{-4} M Eosin-Y in H_2O	8.84 2.81 0.270[2] varying amounts[3]	Rachel Bukowski's thesis	1 hour
TEOS	4.82	DI Water 1.0 M HCl 5.0×10^{-4} M Eosin-Y in H_2O	1.40 0.100 varying amounts[3]	Natasha Eckert's thesis	Overnight
TMOS	4.24	Methanol DI Water 1.5 M NH_4OH 5.0×10^{-4} M Eosin-Y in H_2O	13.7 2.1 0.067 varying amounts[3]	Ben Gauthier	10 minutes

[1] DI water = deionized water.
[2] Originally Bukowski's recipe called for 0.090 mL of 1.0 M HCl. However, it was found that adding more acid improved the recipe. When only 0.090 mL of the 1.0 M HCl was added, the solution was cloudy. Because xerogels are intended to be optically clear a cloudy sol-gel starting solution was not conducive to the experiment.
[3] 5 μL to 50 μL of Eosin-Y was added depending on the desired concentration.

Table II. Recipe for the preparation of the $Ru(bpy)_3^{2+}$-doped xerogels

Precursors	Amounts Used (mL)	Solvents	Amounts Used (mL)	Recipe Obtained from	Time Allowed for Stirring
TMOS	8.5	Methanol DI Water 1.5M NH_4OH varying concentrations[4] $Ru(bpy)_3^{2+}$ in H_2O	27.5 3.6 4 drops 3.6	Smitesh Bakrania	10 minutes

Table III. Recipe for the preparation of the $Ru(bpy)_3^{2+}$-doped aerogels

Precursors	Amounts Used (mL)	Solvents	Amounts Used (mL)	Recipe Obtained from	Time Allowed for Stirring
TMOS	8.5	Methanol DI Water 1.5M NH_4OH varying concentrations $Ru(bpy)_3^{2+}$ in H_2O	27.5 3.6 4 drops 3.6	Smitesh Bakrania	10 minutes

[4] Concentrations of stock solution varied from $1.0x10^{-2}$ M, $1.0x10^{-3}$ M, $1.0x10^{-4}$ M, and $1.0x10^{-5}$ M depending on the desired concentrations.

Table IV. Parameters used for fluorescence excitation spectra

Dye Used	Excitation Wavelength (nm)	Emission Wavelength (nm)
Eosin-Y	500 – 535	545
$Ru(bpy)_3^{2+}$	350 – 580	590

Table V. Parameters used for fluorescence emission spectra

Dye Used	Excitation Wavelength (nm)	Emission Wavelength (nm)
Eosin-Y	525	535 – 650
$Ru(bpy)_3^{2+}$	570	500 – 750

Table VI. Parameters used for fluorescence decay curve

Type	Excitation λ	Emission λ	Scatter λ	Start Delay	End Delay	Channels	Int. time	Averages
With PTI LS-100 Fluorescence Luminescence System								
Aerogel	337 nm	590 nm	337 nm	100 ns	400 ns	100	0.1 s	50
Xerogel	337 nm	590 nm	337 nm	100 ns	400 ns	100	0.1 s	50
With PTI LasterStrobe Fluorescence Lifetime System								
Aerogel	446 nm	540 nm	446 nm	0 ns	1500 ns	400	50 µs	50
Xerogel	446 nm	540 nm	Not needed	0 ns	8000 ns	75	50 µs	1

Table VII. Recipe for the preparation of Eosin-Y-doped sol-gel solution for pin-printing arrays

Precursors	Amounts Used (mL)	Solvents	Amounts Used (mL)	Recipe Obtained from	Time Allowed for Stirring
n-Propyl TMOS TMOS	0.5 0.5	Ethanol DI Water 1.0 M HCl	1.25 0.200 0.040	Rachel Bukowski	1 hour

EXPERIMENTAL WORKS CITED

[1] Hagerman, Michael E., Salamone, Samuel J., Herbst, Robert W., Payeur, Amy L. "Tris(2,2')-bipyridine) ruthenium (II) cations as photoprobes of clay tactoid architecture within hectorite and laponite films." *Chemistry of Materials*, in press.

RESULTS

The results sections is split in two parts: (1) the results of the experiments performed with Eosin-Y and (2) the results of the experiments performed with $Ru(bpy)_3^{2+}$.

EOSIN-Y RESULTS

Results for the preparation of Eosin-Y-doped xerogels, the preparation of Eosin-Y-doped aerogels, excitation and emission spectra, UV/visible absorption spectra, time-based fluorescence scans, and the experiments that were performed at the University of Buffalo are included below.

Preparation of Eosin-Y-Doped Xerogels

Of the three recipes used to prepare Eosin-Y-doped xerogels, only two worked well. The recipe using n-Propyl TMOS and TMOS as its precursors did not yield usable xerogels. The solutions never formed the gels. Although the other two recipes worked well, the recipe using TMOS as its precursor formed xerogels faster. The TMOS recipe required only three days for the monoliths to pull away from the walls of the cuvettes, whereas the TEOS recipe created monoliths that took several weeks to pull away.

Preparation of Eosin-Y-Doped Aerogels

Unfortunately, Eosin-Y proved to be a bad choice for doping aerogels. When the aerogels were received, they were yellow-brown, not the normal pink-orange color of Eosin-Y. After fluorescence and absorption spectra were taken and enormous shifts were noted, it was concluded that the dye had decomposed into an entirely different species.

Excitation and Emission Spectra

The Eosin-Y-doped sol gels formed via the recipe containing the TEOS precursor and the recipe containing the TMOS precursor both had peak fluorescence intensity at approximately the same wavelengths in excitation and emission spectra. The Eosin-Y-doped sol-gel solutions and wet and dry xerogels have excitation maxima of 523 to 531 nm. Figure 6 contains excitation spectra for TEOS sol-gels of varying Eosin-Y concentrations that display maximum excitation wavelengths of 530 nm. Figure 7 is excitation spectra for TMOS sol-gels of varying concentrations that display intensity peaks at a maximum wavelength of 523 nm. The Eosin-Y-doped sol-gel solutions and xerogels for these two recipes when excited at 525 nm resulted in emission spectra at maximum wavelengths of 543 to 550 nm. Emission spectra for TEOS sol-gels of varying concentrations are shown in Figure 8 with peaks at a maximum wavelength of 550 nm. Figure 9 displays emission spectra for TMOS sol-gels of varying concentrations with peaks at a maximum wavelength of 545 nm.

The recipe containing both n-Propyl TMOS and TMOS precursors produced different results than the other two recipes for both excitation and emission spectra. Excitation maxima of 471 to 476 nm and emission maxima of 551 to 554 nm were observed. The spectra for the n-Propyl TMOS/TMOS mixtures were only taken in solution form since the solutions failed to ever form xerogels.

The spectra of the aerogels showed a significant shift from the other Eosin-Y-doped materials. The aerogels were excited at a maximum wavelength of 316 nm, as seen in Figure 10, and they emitted at a maximum wavelength of 396 nm, as seen in Figure 11. These values were much lower than the observed peaks for Eosin-Y-doped xerogels and sol-gel solutions.

In all excitation and emission spectra, the more concentrated the sample, the higher its fluorescence intensity was. For Eosin-Y in solution, excitation maxima of 523 to 532 nm and emission maxima of 545 to 550 nm were observed.

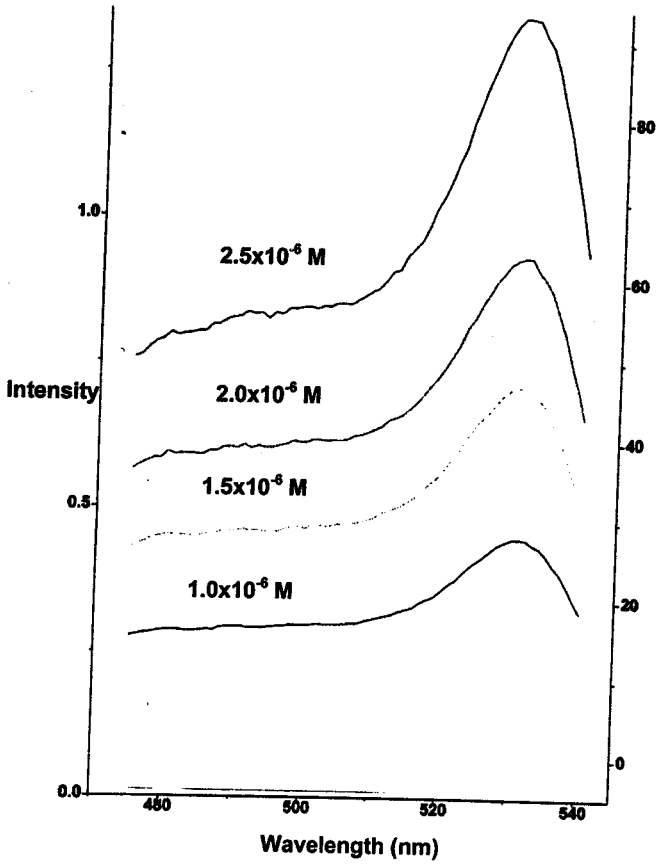

Figure 6. Corrected excitation spectra of TEOS sol-gels of varying concentrations (λ_{max} = 530 nm), λ_{em} = 550 nm, λ_{ex} = 475 nm – 540 nm, $slit_{em}$ = 4 nm, $slit_{ex}$ = 4 nm

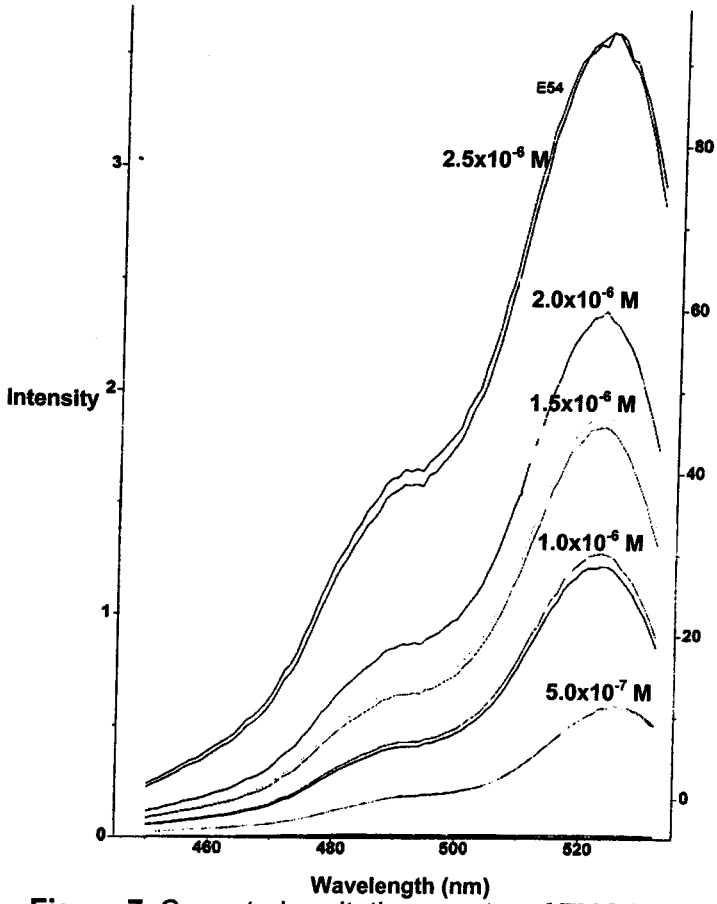

Figure 7. Corrected excitation spectra of TMOS sol-gels of varying concentrations (λ_{max} = 523 nm), λ_{em} = 542 nm, λ_{ex} = 450 nm – 532 nm, $slit_{em}$ = 2 nm, $slit_{ex}$ = 2 nm

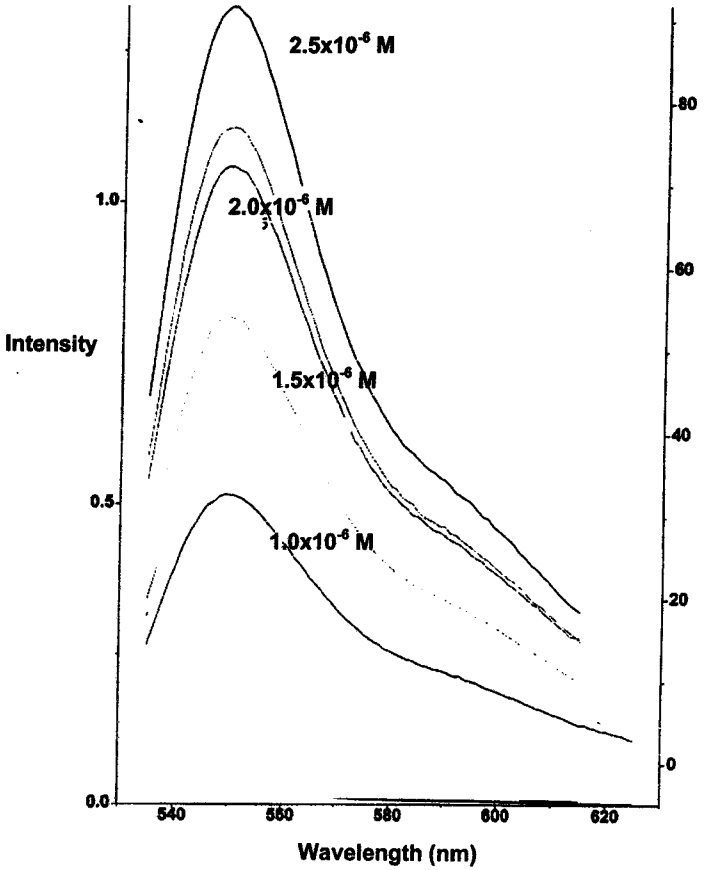

Figure 8. Corrected emission spectra of TEOS sol-gels of varying concentrations (λ_{max} = [illegible] nm), λ_{em} = 535 nm – 615 nm, λ_{ex} = 525 nm, $slit_{em}$ = [illegible], $slit_{ex}$ = 4 nm

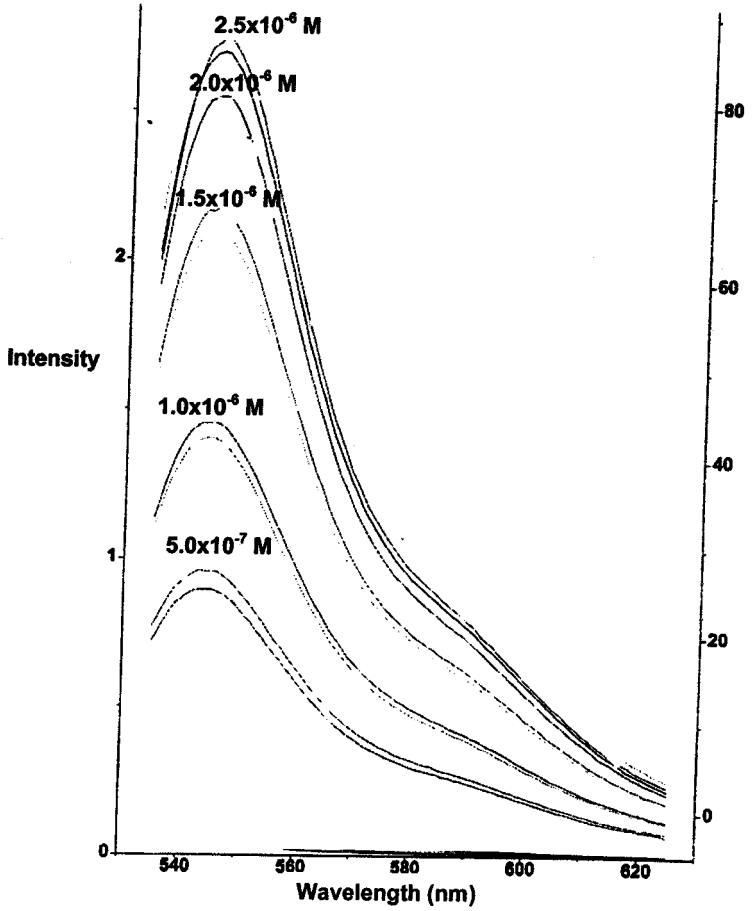

Figure 9. Corrected emission spectra of TMOS sol-gels of varying concentrations (λ_{max} = 545 nm), λ_{em} = 535 nm – 625 nm, λ_{ex} = 525 nm, $slit_{em}$ = 4 nm, $slit_{ex}$ = 4 nm

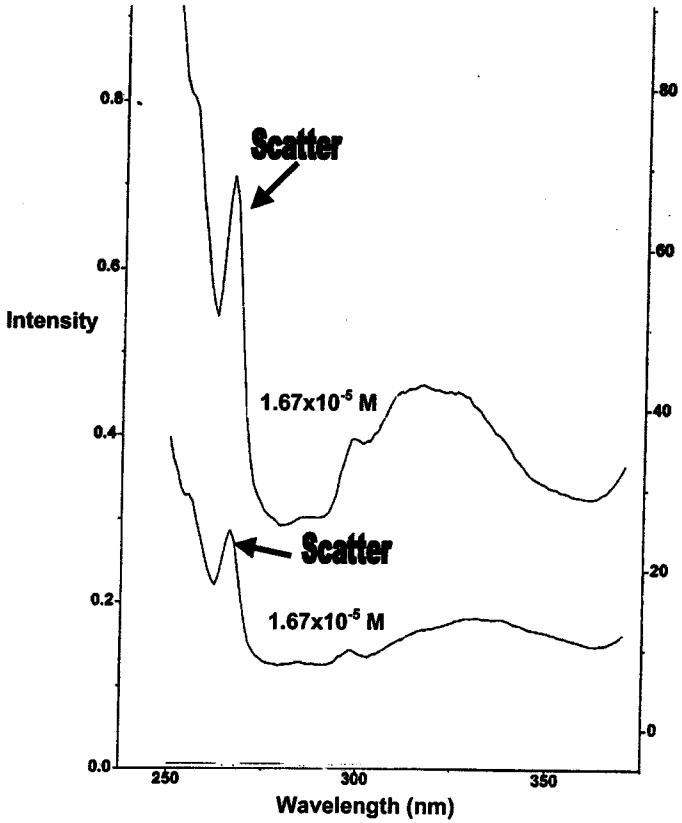

Figure 10. Corrected excitation spectra of aerogels (λ_{max} = 316 nm), λ_{em} = 380 nm, λ_{ex} = 250 nm – 370 nm, $slit_{em}$ = 4 nm, $slit_{ex}$ = 4 nm

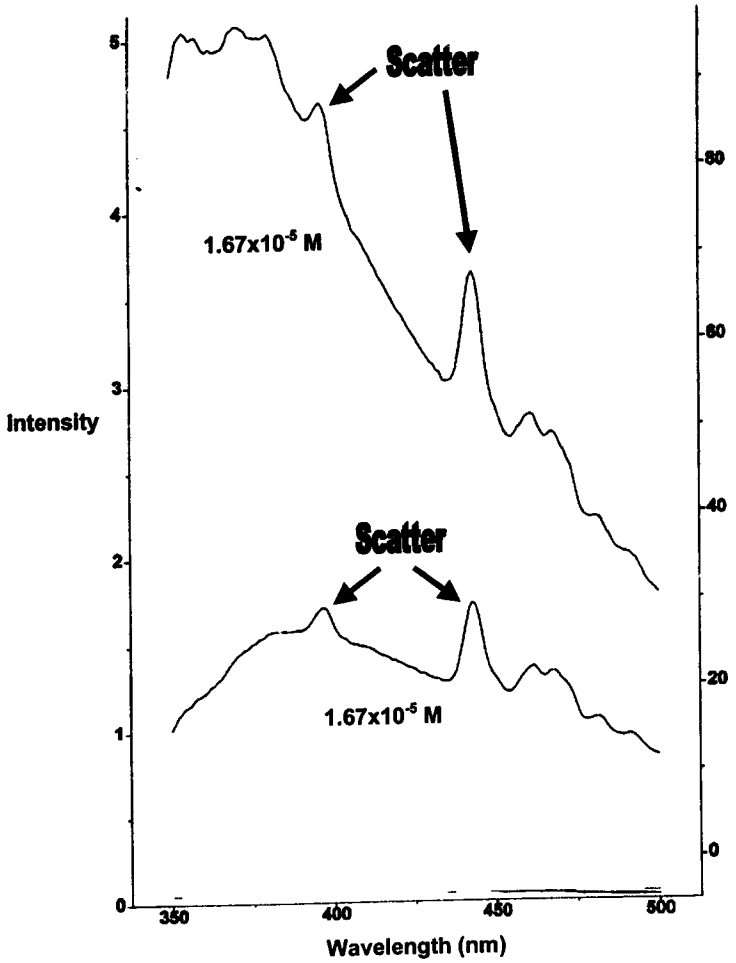

Figure 11. Corrected emission spectra of aerogels (λ = 396 nm), λ_{em} = 350 nm – 500 nm, λ_{ex} = 310 nm, $slit_{em}$ = 4 nm, $slit_{ex}$ = 4 nm

UV/Visible Absorption Spectra

The xerogels and sol-gel solutions from the recipe using the TMOS precursor were the only samples that could be accurately examined in terms of absorption. The other two recipes, one involving the TEOS precursor and the other involving the n-Propyl TMOS/TMOS precursors were not colored enough to absorb significantly. The TMOS precursor absorbed maximally between 523 and 531 nm, as can be seen in Figure 12. As expected, all of the absorption spectra of the samples tested concurred with their corresponding excitation spectra. Eosin-Y in solution was determined to absorb maximally between 517 and 536 nm. In the absorption spectra for the aerogels doped with Eosin-Y (seen in Figure 13), a peak was observed for all three samples at approximately 308 nm, much lower than the observed peaks for the Eosin-Y-doped xerogels and sol-gel solutions. The aerogel absorption spectra are very noisy due to a lot of scattering and a consequently small transmission signal. The more concentrated samples absorbed more intensely, and vice versa.

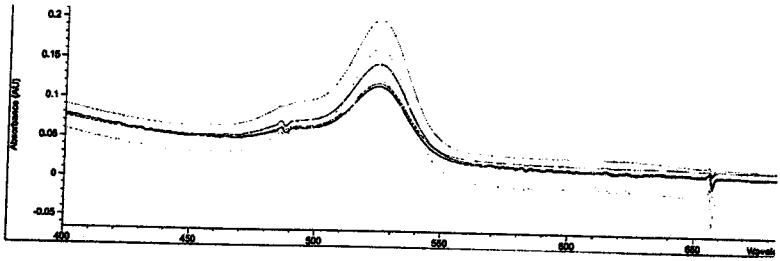

Figure 12. UV/Visible absorption spectra of TMOS sol-gels of varying concentrations (λ_{max} = 530 nm)

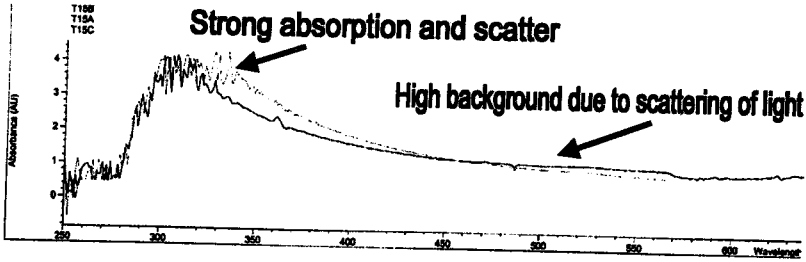

Figure 13. UV/Visible absorption spectra of aerogels of varying concentrations (λ_{max} ≈ 308 nm)

Steady-State Time-Based Scans

The time-based fluorescence scans for the Eosin-Y-doped xerogels, shown here in Figure 14, demonstrated that Eosin-Y was in fact a pH sensor that could maintain its functionality while trapped in the xerogel. The time-based scans were done over periods of two hours because of the lengthy response times required for intensity changes. When acid was added the fluorescence intensity decreased and when base was added the fluorescence intensity increased, as expected.

The Eosin-Y-doped xerogels were able to maintain their abilities as pH detectors by allowing the H_3O^+ and OH^- ions to diffuse into the xerogels. When the pH was altered by either adding 0.1 M HCl or 0.1 M NaOH, there were significant changes in fluorescence intensity. After acid was added and the fluorescence intensity dropped, by adding base the fluorescence intensity was able to return to its original level, showing that the Eosin-Y-doped xerogels could be used as reversible detectors.

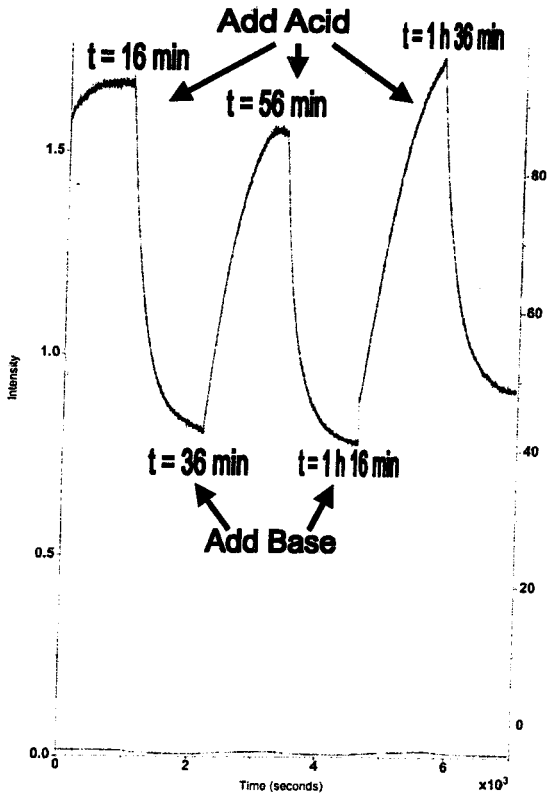

Figure 14. Time-based scan of Eosin-Y-doped xerogel as aliquots of 0.1 M HCl and 0.1M NaOH were added

State University of New York Buffalo Research

The University of Buffalo research resulted in the creation of Eosin-Y-doped sol-gel pin-printed slides. After exciting the slides with a He/Cd laser the images of the sol-gel material fluorescing on the slides were projected from a CCD camera to a computer screen. The slides displayed images of the Eosin-Y-doped sol-gel materials fluorescing in air as seen in Figure 15. When the slides were flooded with 0.1M HCl, the fluorescence went down as was expected, which can be seen in Figure 16. However, when the slides were then flooded with 0.01M NaOH to test their reversibility in indicating pH changes, the fluorescence did not go return to its original intensity level as expected. This is probably due to the lack of drying time allowed for the slides.

Figure 15. Fluorescing image of pin-printed slide with Eosin-Y-doped sol-gel array in air

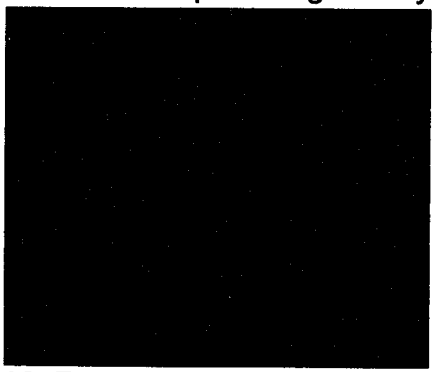

Figure 16. Fluorescing image of pin-printed slide with Eosin-Y-doped sol-gel array in 0.1 M HCl

$Ru(bpy)_3^{2+}$ RESULTS

The results from the preparation of $Ru(bpy)_3^{2+}$-doped xerogels, the preparation of $Ru(bpy)_3^{2+}$-doped aerogels, excitation and emission spectra, and fluorescence lifetime decay curves are shown below.

Preparation of $Ru(bpy)_3^{2+}$-Doped Xerogels

The preparation of xerogels was performed by the mechanical engineers in the project using the recipe from the experimental section. $Ru(bpy)_3^{2+}$ was successfully entrapped in xerogels.

Preparation of $Ru(bpy)_3^{2+}$-Doped Aerogels

$Ru(bpy)_3^{2+}$, unlike Eosin-Y, was successfully entrapped in aerogels. The molar concentrations of stock solution that worked for the aerogels were $1.0x10^{-5}$ M, $1.0x10^{-4}$ M, and $1.0x10^{-3}$ M. Optically transparent aerogels at higher concentrations could not be obtained in the current aerogel fabrication process, and lower concentrations did not give sufficient fluorescence signal for measurements.

Excitation and Emission Spectra

Figure 17 shows that in emission spectra, $Ru(bpy)_3^{2+}$-doped xerogels fluoresced at a maximum wavelength of 590 nm. The emission spectra for $Ru(bpy)_3^{2+}$-doped aerogels, which can also be seen in Figure 17, show that the $Ru(bpy)_3^{2+}$ entrapped in aerogels fluoresced at maximum wavelengths of 598 nm to 604 nm. In excitation spectra, seen in Figure 18, $Ru(bpy)_3^{2+}$-doped xerogels and aerogels have excitation maxima between 454 nm and 478 nm. $Ru(bpy)_3^{2+}$-doped aerogels and xerogels also show a shoulder at 420 nm.

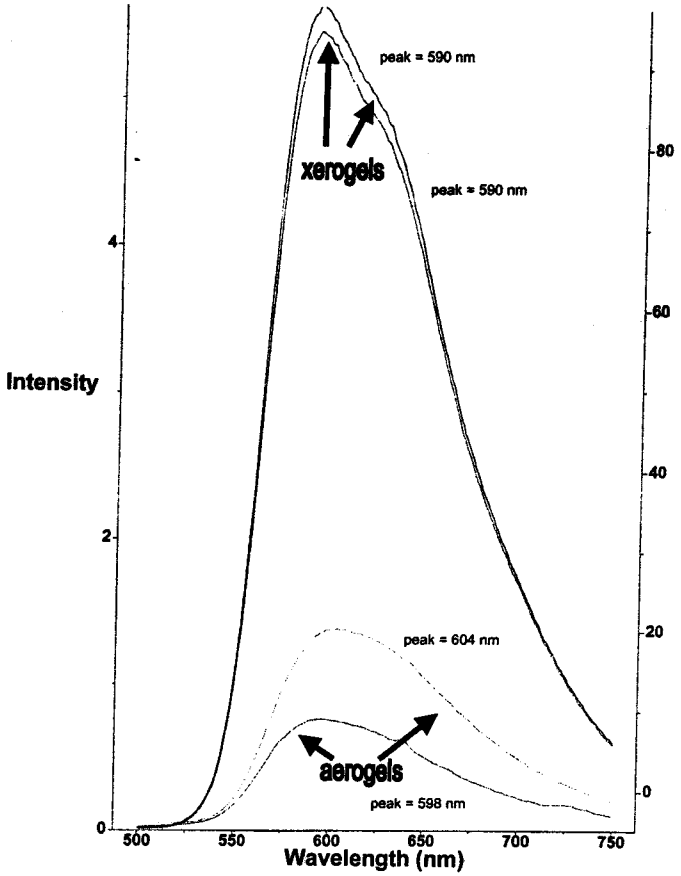

Figure 17. Corrected emission spectra for $Ru(bpy)_3^{2+}$-doped aerogels and xerogels with concentrations within the gels of $1.0x10^{-3}$ M (λ_{max} = 590 nm to 604 nm), λ_{em} = 500 nm – 750 nm, λ_{ex} = 452 nm, $slit_{em}$ = 2 nm, $slit_{ex}$ = 4 nm

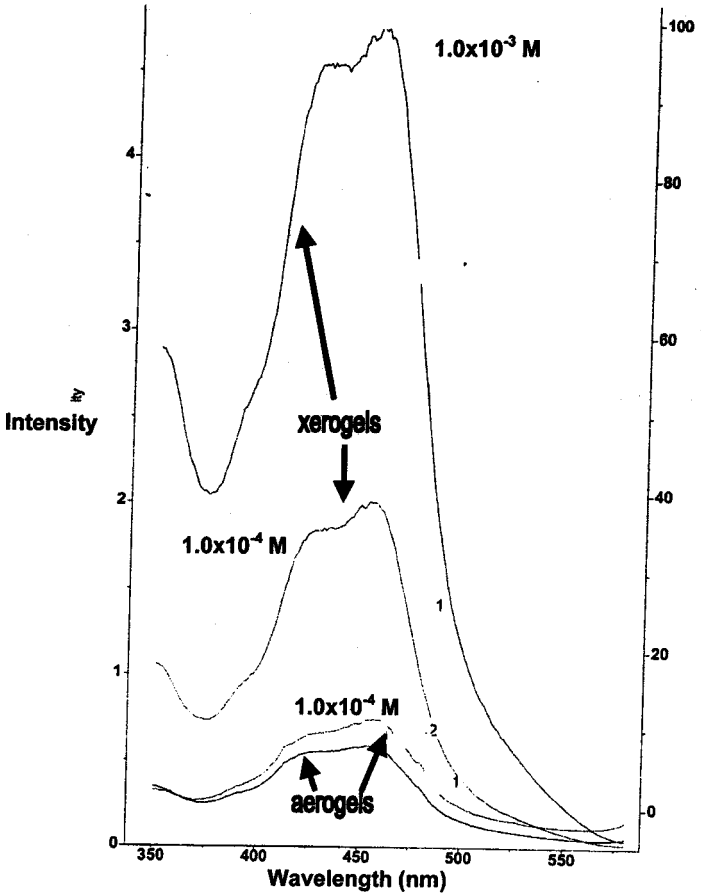

Figure 18. Corrected excitation spectra for $Ru(bpy)_3^{2+}$-doped aerogels and xerogels of varying concentrations within the gels(λ_{max} = 470 nm), λ_{em} = 590 nm, λ_{ex} = 350 nm – 575 nm, $slit_{em}$ = 4 nm, $slit_{ex}$ = 4 nm

UV/Visible Absorption Spectra

Figure 19 shows the absorption spectra of $Ru(bpy)_3^{2+}$-doped xerogels and $Ru(bpy)_3^{2+}$-doped aerogels. Both materials show maximum absorbance values at 454 nm with shoulders at 420 nm.

Fluorescence Lifetime Decay Curves

Figure 20 shows the fluorescence lifetime decay curves for $Ru(bpy)_3^{2+}$-doped xerogels. The lifetime data for these xerogels can be seen in Table VIII. The $Ru(bpy)_3^{2+}$-doped xerogels were found to have two-exponential lifetime decays. The proportion of the two lifetimes occurring is roughly 50:50. Figure 21 shows the fluorescence lifetime decay curves for $Ru(bpy)_3^{2+}$-doped aerogels. The lifetime data for these aerogels can also be seen in Table VIII. The $Ru(bpy)_3^{2+}$-doped aerogels were determined to also have two-exponential lifetime decays, however in the case of the doped aerogels, the shorter lifetime dominated. The percentage of the first, shorter lifetime is approximately 85%.

Aerogels as Oxygen Sensors

$Ru(bpy)_3^{2+}$-doped aerogels show success in acting as oxygen sensors which can be seen in Figure 22. When the aerogels are allowed to be in contact with air, which of course contains O_2, they display a steady fluorescence intensity. However, when the aerogels are flooded with nitrogen gas, the intensity immediately increases with a response time of about two seconds. Once the N_2 gas is turned off, and the aerogel is exposed to air again, the fluorescence intensity returns to its original level. This change in

fluorescence intensity demonstrates that the $Ru(bpy)_3^{2+}$ entrapped in the aerogel is being quenched by oxygen. Thus, the $Ru(bpy)_3^{2+}$-doped aerogels can be used as O_2 sensors.

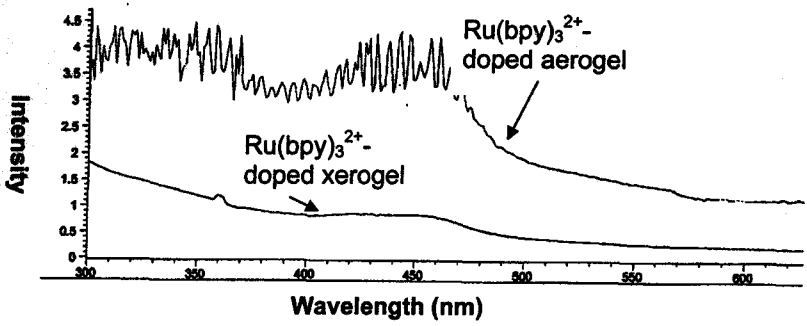

Figure 19. UV/Visible absorption spectra of a $Ru(bpy)_3^{2+}$-doped aerogel and a $Ru(bpy)_3^{2+}$-doped xerogel (λ = 454 nm)

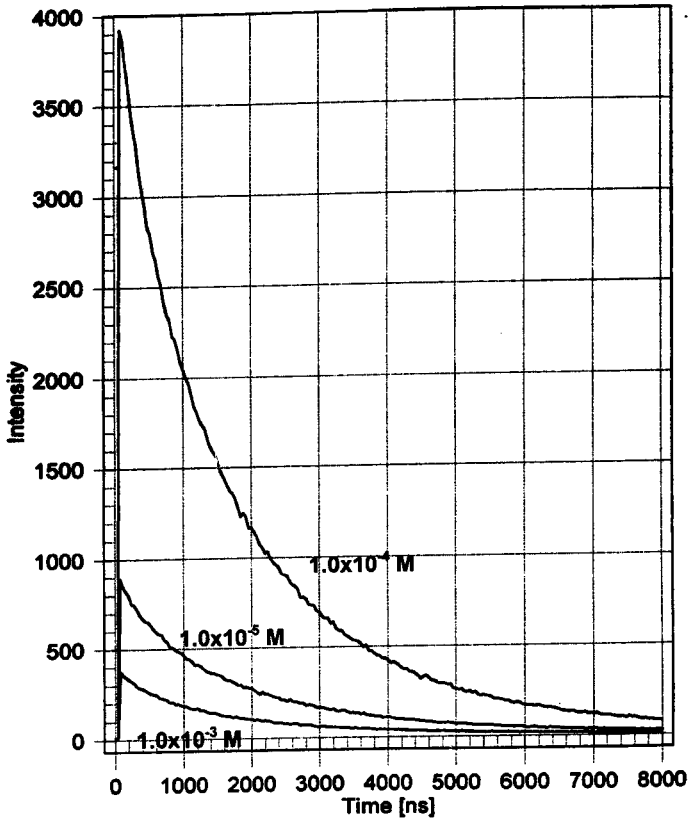

Figure 20. Fluorescence decay curve for $Ru(bpy)_3^{2+}$-doped xerogels of varying concentrations, λ_{em} = 590 nm, λ_{ex} = 446 nm, 20 averages each

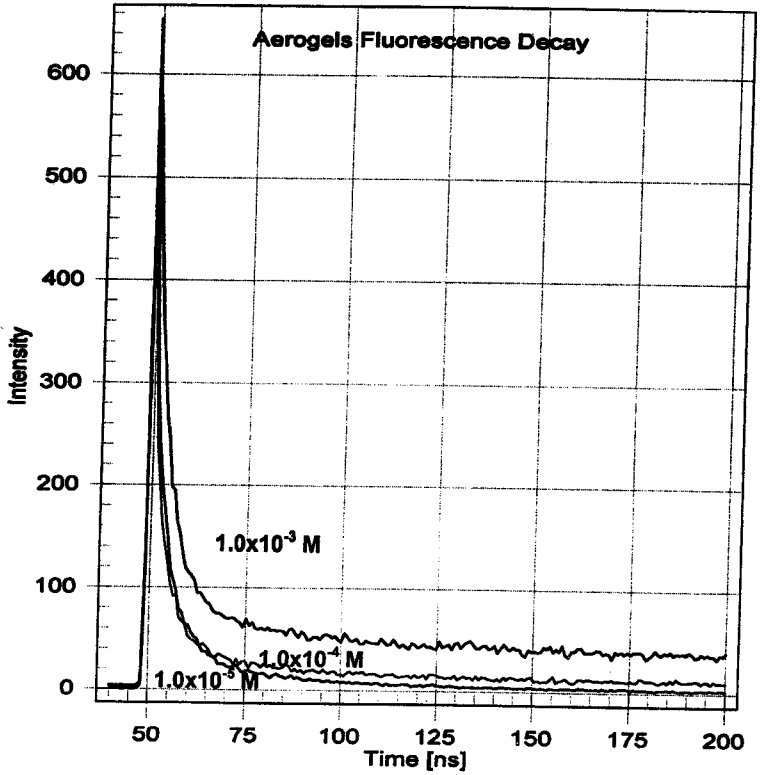

Figure 21. Fluorescence decay curve for $Ru(bpy)_3^{2+}$-doped aerogels of varying concentrations, λ_{em} = 590 nm, λ_{ex} = 446 nm, 1 average each

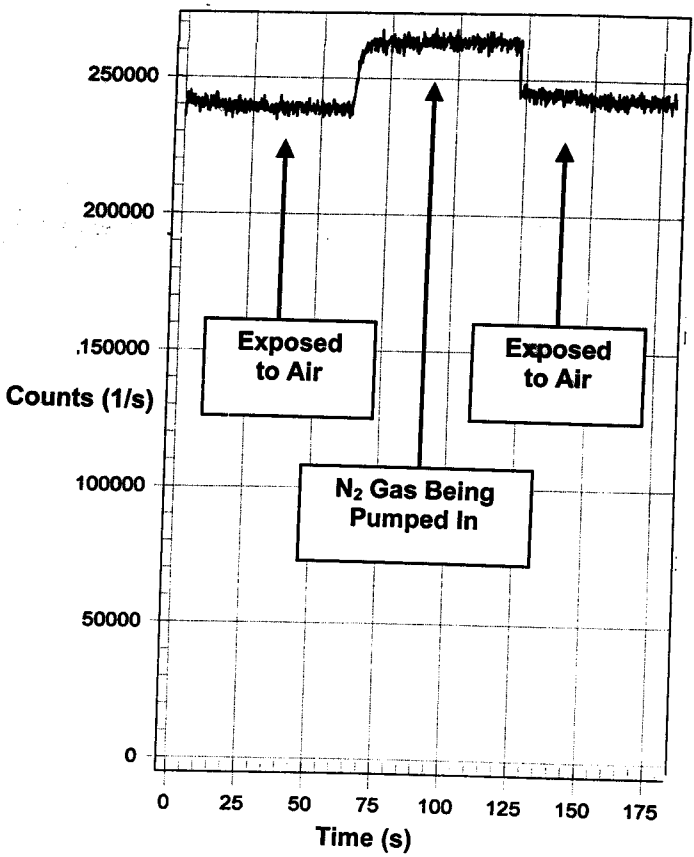

Figure 22. Fluorescence time-based scan with $Ru(bpy)_3^{2+}$-doped aerogel with $1.0x10^{-4}$ M concentration in the gel

Table VIII. Fluorescence lifetime decay data for $Ru(bpy)_3^{2+}$-doped xerogels and $Ru(bpy)_3^{2+}$-doped aerogels of varying concentrations.

Type	$[Ru(bpy)_3^{2+}$ Solution] (M)	τ_1 (μs)	A_1	τ_2 (μs)	A_2	χ^2
Xerogel	1.0×10^{-3}	2.5 ± 0.1	55 ± 5 %	0.94 ± 0.79	45 ± 4 %	0.9446
Xerogel	1.0×10^{-4}	2.1 ± 0.5	65 ± 3 %	0.90 ± 0.56	35 ± 3 %	0.9861
Xerogel	1.0×10^{-5}	2.2 ± 0.1	53 ± 5 %	0.81 ± 0.74	47 ± 5 %	0.9566
Aerogel	1.0×10^{-3}	0.0041 ± 0.0002	85 ± 7 %	0.92 ± 0.30	15 ± 1 %	1.059
Aerogel	1.0×10^{-4}	0.0047 ± 0.002	79 ± 7 %	0.91 ± 0.30	21 ± 1 %	1.073
Aerogel	1.0×10^{-5}	0.0064 ± 0.002	88 ± 4 %	1.1 ± 0.2	12 ± 1 %	0.9764

τ_1 and τ_2 represent the first and second lifetimes respectively, A_1 and A_2 represent the first and second exponential percentages respectively, and χ^2 represents the accuracy of the fit ($\chi^2 = 1$ denotes a perfect fit).

DISCUSSION

EOSIN-Y DISCUSSION

The data for Eosin-Y-doped xerogels is conclusive and somewhat expected, however the data for the Eosin-Y-doped aerogels is more disappointing.

Among the expected results, the excitation spectra of Eosin-Y-doped sol-gel solutions and xerogels are similar to their UV/Visible absorption spectra (Figures 6, 7, and 12). Also, the excitation, emission, and UV/Visible absorption spectra of Eosin-Y in solution compared to Eosin-Y in xerogels for both TEOS and TMOS precursors do not change (Figures 6 - 9). These corresponding spectra demonstrate that the electronic properties of Eosin-Y are not affected significantly by immobilization of the species in the sol-gel matrix. The time-based scans of Eosin-Y-doped xerogels show that they are in fact reversible pH sensors (Figure 14) but response times are relatively long, approximately 20 minutes, which is a disadvantage. The reason for the long response time of Eosin-Y entrapped in sol-gel material acting as a pH indicator is because the H_3O^+ and OH^- ions must diffuse into the monolith to react with Eosin-Y.

In contrast, the Eosin-Y-doped aerogels produce unusual results. The excitation and emission spectra for Eosin-Y-doped aerogels appear much differently than the doped xerogels, mostly consisting of scattering (Figures 10 and 11). Also, the UV/visible absorption spectra for Eosin-Y-doped aerogels show maxima around 308 nm, more than 200 nm less than Eosin-Y-

doped xerogels (Figure 13). The most likely explanation for why the Eosin-Y in aerogels seems to have decomposed into a completely different species is that the Eosin-Y is unable to withstand the high temperatures of the aerogel fabrication process.

Initial tests of Eosin-Y-doped pin-printed microsensors are inconclusive. The reason for the lack of success in preparing reversible sensors with the pin-printed slides is due to the notably shortened aging period. Instead of the usual two weeks, the two days that the slides were allowed to age is not enough time for the sol-gel material to fully dry on and adhere to the slides. Consequently, when the slides are flooded with solvent, the printed arrays are actually being washed off. Thus, when the fluorescence decreases after the 0.1M HCl is added (Figure 16), it may actually not be due to the pH levels going down, but instead to the fact that some of the material is no longer on the slide. This washing off explains why after increasing the pH of the solution in contact with the microsensor array, the fluorescence still does not increase as would be expected.

FUTURE WORK WITH EOSIN-Y

An advantage of microsensors over xerogels is that they are likely to have much faster response times to changes in pH than the monoliths because there is less distance for the analyte to diffuse in microsensors. For future work, the research with microsensors should be explored more extensively. The Eosin-Y-doped sol-gel microsensors would probably have given better results had the slides had more time to dry.

Continued research with the monoliths would give more insight to how long Eosin-Y continues to work as a reversible sensor while entrapped in sol-gel material.

Eosin-Y appears to be unsuitable as a probe for the comparison of species entrapped in xerogels and aerogels, because it does not survive the high temperatures of the aerogel fabrication process.

$Ru(bpy)_3^{2+}$ DISCUSSION

$Ru(bpy)_3^{2+}$, unlike Eosin-Y, can successfully be entrapped in aerogels. The emission spectra for $Ru(bpy)_3^{2+}$-doped aerogels and xerogels show significant blue shifts at their maximum peaks. The known values for $Ru(bpy)_3^{2+}$ maximum emission spectrum wavelengths for $Ru(bpy)_3^{2+}$ in water and in sol gel form are 610 nm and 620 nm, respectively[1]. The emission spectra obtained experimentally from $Ru(bpy)_3^{2+}$-doped aerogels and xerogels showed maxima at 590 to 604 nm (Figure 17). The shifts can be contributed to emission from the triplet metal-to-ligand charge transfer from the excited state to the ground state[1]. The blue shifts observed also show that there is a less fluid guest microenvironment in $Ru(bpy)_3^{2+}$-doped xerogels and aerogels, suggesting that little to no water is present in the xerogels and aerogels[2]. The $Ru(bpy)_3^{2+}$-doped xerogels and aerogels have excitation maxima at approximately the same wavelengths as the absorbance maxima (Figures 18 and 19). The peak and the shoulder observed in both the excitation and absorption spectra are due to metal-to-ligand charge transfer ($t_{2g}(Ru) \rightarrow \Pi^*(bpy)$) transitions[1].

The fluorescence lifetime data for the $Ru(bpy)_3^{2+}$-doped aerogels and xerogels give informative results on the microenvironments present in the aerogels and xerogels (Table VIII). The lifetime data for the $Ru(bpy)_3^{2+}$-doped aerogels show that the $Ru(bpy)_3^{2+}$ entrapped in the aerogels demonstrate a major, very short fluorescent lifetime of approximately 0.0050 μs representing approximately 85% of the system. There is also evidence of a minor and

much longer second lifetime of approximately 0.98 μs representing approximately 15% of the system. The minor, second lifetime of the $Ru(bpy)_3^{2+}$-doped aerogels is approximately equal to the minor, second lifetime of the $Ru(bpy)_3^{2+}$-doped xerogels indicating a similar microenvironment present in both. The second lifetime in this case is approximately 0.88 μs and represents approximately 42% of the system. The first lifetime of the $Ru(bpy)_3^{2+}$-doped xerogels is again the major fluorescent lifetime and is about five hundred times larger than that of the major first lifetime of the $Ru(bpy)_3^{2+}$-doped aerogels. This first lifetime for the doped xerogels is approximately 2.3 μs, representing 58% of the total system. The fact that both $Ru(bpy)_3^{2+}$-doped xerogels and aerogels show two lifetimes, one major and one minor, is evidence that in both cases, the $Ru(bpy)_3^{2+}$ species are entrapped in two different microenvironments within the gels.

The ability for $Ru(bpy)_3^{2+}$ to relax once excited is strongly affected by the solvent surrounding the species. The fluorescence lifetime data signifies that the microenvironments around the fluorescing $Ru(bpy)_3^{2+}$ are not the same in xerogels and aerogels. A long fluorescence lifetime is characteristic of a species with a more fluid microenvironment, whereas a short lifetime is a property of a species with a less fluid environment[1]. The significance of the xerogel lifetime fluorescence data, which gives two long lifetimes, is that there is little to no "external $Ru(bpy)_3^{2+}$" present in the $Ru(bpy)_3^{2+}$-doped xerogels. Instead, the data suggests that all the $Ru(bpy)_3^{2+}$ are trapped within more fluid microenvironments. The shorter lifetimes observed in the $Ru(bpy)_3^{2+}$-doped

aerogels demonstrate how the $Ru(bpy)_3^{2+}$ are trapped within a much less fluid microenvironment. There is (theoretically) no solvent in the aerogels, whereas there is a small amount of solvent in the xerogels. The $Ru(bpy)_3^{2+}$ that is trapped in aerogels, is actually trapped to the Si-O walls.

The results from the O_2 sensor research successfully demonstrated that $Ru(bpy)_3^{2+}$ aerogels can be used as O_2 sensors. The response time of the aerogels as O_2 sensors are very quick, on the order of several seconds (Figure 22). It should be noted that the lifetimes should be measured in the absence of oxygen because the observed lifetimes were likely shortened from the "natural" lifetimes due to oxygen quenching.

FUTURE WORK WITH $Ru(bpy)_3^{2+}$

Future work should include reexamining the lifetimes of $Ru(bpy)_3^{2+}$-doped xerogels and aerogels in the absence of oxygen. It should also incorporate entrapping other dyes with interesting electronic properties into aerogels, including other ruthenium complexes, to examine their abilities as sensors. Additionally, it would be interesting to create and evaluate $Ru(bpy)_3^{2+}$-doped pin-printed microsensors. It would then be possible to compare the response times as sensors of the doped microsensors to the doped aerogels.

DISCUSSION WORKS CITED

[1] Innocenzi, Plinio, Kozuka, Hiromitsu, and Yoko, Toshinobu. "Fluorescence Properties of the $Ru(bpy)_3^{2+}$ Complex Incorporated in Sol-Gel-Derived Silica Coating Films. *J. Phys. Chem. B*, 1997, 101, 2285-2291.

[2] Hagerman, Michael E., Salamone, Samuel J., Herbst, Robert W., Payeur, Amy L. "Tris(2,2'-bipyridine) ruthenium (II) cations as photoprobes of clay tactoid architecture within hectorite and laponite films." *Chemistry of Materials*, in press.